A Simple Strategy to Address Imbalanced Long-tail Classification Accuracies (TODO: rethink title)

Nadine Chang[1,*] Jayanth Koushik[1,*] Michael J. Tarr[1]
Martial Hebert[1] Yu-Xiong Wang[2]

Abstract

Methods in long-tail learning focus on improving performance for data-poor (rare) classes; however, performance for such classes remains much lower than performance for more data-rich (frequent) classes. Analyzing the predictions of long-tail methods on rare classes reveals that a large number of errors are due to misclassification of rare items as visually similar frequent classes. To address this problem, we introduce AlphaNet, a method that can be applied to existing models, performing *post hoc* correction on classifiers of rare classes. Starting with a pre-trained model, we find frequent classes that are closest to rare classes in the model's representation space and learn weights to update rare classifiers with a linear combination of frequent classifiers. AlphaNet, applied on several different models, greatly *improves test accuracy for rare classes* in multiple long-tail datasets. We then analyze predictions from AlphaNet and find that remaining errors are to often due to separations among semantically similar classes. Evaluating with semantically similar classes grouped together, AlphaNet also *improves overall accuracy*, showing that the method is practical for long-tail classification problems.

1 Introduction

Objects in the real world follow a long-tailed distribution, where many categories occur only rarely[?]. Due to this phenomenon, many computer vision applications require models that can learn to accurately classify rarer objects alongside common ones. For example, autonomous vehicle systems are expected to classify rare animals, objects, or road configurations in order to avoid potential collisions[?]; medical image analysis systems should spot rare cancers, detect unusual anatomical irregularities, and reconstruct images from few examples[?]. To address challenges in these and related use cases, we focus on object classification using long-tailed datasets – "long-tail classification".

The significance of long-tailed distributions in real-world applications has spurred a variety of approaches for long-tail classification. Learning in this setting is challenging because many classes are "rare" – having only a small number of samples. Some methods re-sample more data for rare classes in an effort to address data imbalance[?]. Other methods adjust learned classifiers to re-weight them in favor of rare classes[?]. Both re-sampling and re-weighting methods provide strong

*Equal contribution. [1]Carnegie Mellon University. [2]University of Illinois at Urbana-Champaign.
Email: nchang1@cs.cmu.edu, jkoushik@andrew.cmu.edu, michaeltarr@cmu.edu, hebert@cs.cmu.edu, yxw@illinois.edu.

baselines for long-tail classification tasks. However, state-of-the-art results are achieved by more complex methods that, for example, learn multiple experts[?], perform multi-stage distillation[?], or use a combination of weight balancing, data re-sampling, and loss decay[?].

Despite these advances, accuracy on rare classes continues to be significantly worse than overall accuracy. For example, on the ImageNet-LT dataset, the expert model of **?** (**?**)[?] has an average accuracy of xx.x% on frequent classes, but an average accuracy of xx.x% on rare classes. In addition to significantly reducing overall accuracy, such performance imbalances raise ethical concerns in contexts where unequal accuracy leads to biased outcomes, for instance as in medical image computing[?] (TODO: find other instances of bias). For these reasons, our method is aimed at directly improving the accuracy for rare classes in long-tail classification.

1.1 Analysis

Notation: Throughout this work, we will define the distance between two classes as the distance between their average training set representation. Given a classification model, let f be the function mapping images to vectors in $\mathbb{R}^d$ (typically, this is the output of the penultimate layer in convolutional networks). For a class c with training samples $I_1^c, ..., I_{n_c}^c$, let $x^c \equiv (1/n_c) \sum_i f(I_i^c)$. Given a distance metric $\mu : \mathbb{R}^d \times \mathbb{R}^d \to \mathbb{R}$, for classes c_1 and c_2, we define $m_\mu(c_1, c_2) \equiv \mu(x^{c_1}, x^{c_2})$.

To understand the poor rare class performance of long-tail models, we analyzed the predictions of the 'routing diverse experts' (RIDE) model[?] on 'few' split test samples in ImageNet-LT. The 'few' split is comprised of classes with less than 20 training samples (note that at test time, all classes have 50 samples), and as noted earlier, the RIDE model achieves an accuracy of xx.xx% on this split. To categorize predictions, for each class in the 'few' split of ImageNet-LT, we found the 10 nearest neighbors in the 'base' split (all classes not in the 'few' split) using Euclidean distance ($\mu(a, b) = \|a - b\|$) between features from the RIDE model. For any class, we will refer to its nearest neighbors as visually similar classes. Figure **??** shows predictions on the test set binned into three groups: 1) samples predicted correctly, 2) samples incorrectly predicted as a visually similar class (e.g., predicting 'husky' instead of 'malamute'), and 3) samples incorrectly predicted as a visually dissimilar class (e.g., predicting 'camel' instead of 'malamute'). We can see that a significant portion of the misclassifications (about xx% in this case) are to visually similar classes. Figure **??** shows samples from one pair of visually similar classes; the differences are subtle, and can be hard even for humans to identify.

To make the influence of visually similar classes concrete, we next analyzed the relationship between test accuracy and mean nearest neighbor distance (i.e., the average m_μ between a class and its nearest neighbors). This is shown in Figure **??**, where we can see a strong positive correlation between accuracy and mean distance–'few' split classes with close neighbors have smaller test accuracy than classes with distant neighbors.

1.2 Method overview

Based on the previous analysis, we designed a method, AlphaNet, to improve classifiers for rare classes using information from visually similar frequent classes. We will use the term 'classifier' to denote the linear mapping from feature vectors to class scores. For a class c, this is a vector $w_c \in R^d$ (in convolutional networks, the last layer is generally a matrix of all individual classifiers). Given a

feature vector $z = f(I)$ for some image I, $w_c^T z$ is the prediction score for class c (the bias term is omitted here for simplicity), and the model's class prediction for I is given by $\arg\max_c w_c^T f(I)$.

Figure **??** shows the overview of our method. At a high level, AlphaNet can be seen as moving the classifiers for rare classes based on their position relative to visually similar classes. Importantly, it updates classifiers without making any changes to the representation space, or to other classifiers in the model. It performs a post-hoc correction, and as such, is applicable to use cases where existing base classifiers are either unavailable or fixed (e.g., due to commercial interests or data privacy protections). The simplicity of our method lends to computation advantages–AlphaNet can be trained rapidly, and without need for multiple graphics processing units (GPUs).

2 Related work

Combining, creating, modifying, and learning model weights are concepts that have been implemented in many earlier models. As we review below, these concepts appear frequently in transfer learning, meta-learning, zero-shot/low-shot learning, and long-tail learning.

2.1 Classifier creation

The process of creating new classifiers is captured within meta-learning concepts such as learning-to-learn, transfer learning, and multi-task learning [1–5]. These approaches generalize to novel tasks by learning shared information from a set of related tasks. Many studies find that shared information is embedded within model weights, and, thus, aim to learn structure within learned models to directly modify the weights of a different network [6–13]. Other studies go even further and instead of modifying networks, they create entirely new networks exclusively from training samples [14–16]. In contrast, AlphaNet only combines existing classifiers, without having to create new classifiers or train networks from scratch.

2.2 Classifier or feature composition

In various classical approaches, there has been work that learns better embedding spaces for image annotation [17], or uses classification scores as useful features [18]. However, these approaches do not attempt to compose classifiers nor do they address the long-tail problem. Within non-deep methods in classic transfer learning, there have been attempts to use and combine support vector machines (SVMs). In the work of Tsochantaridis et al. (2005) [19], SVMs are trained per object instance, and a hierarchical structure is required for combination in the datasets of interest. Such a structure is typically not guaranteed nor provided in long-tailed datasets. Additional SVM work uses regularized minimization to learn the coefficients necessary to combine patches from other classifiers [20].

While these approaches are conceptually similar to our method, AlphaNet has the additional advantage of *learning* the compositional coefficients without any hyper-parameters and tuning. Specifically, different novel classes will have their own sets of composition coefficients, and similar novel classes will naturally have similar coefficients. Learning such varying sets of coefficients is difficult in previous classical approaches, which either learn a fixed set of alphas for all novel classes or are forced to introduce more complex group sparsity-like constraints. Finally, in zero-shot learning there exist methods which compose classifiers of known visual concepts to learn a completely new

classifier[15,21–23]. However, such composition is often guided by additional attribute supervision or textual description – two factors on which AlphaNet does not depend.

2.3 Learning transformations between models and classes

Other studies have demonstrated different ways of learning transformations to modify model weights in an attempt to learn these transformations with stochastic gradient descent (SGD) optimization[24,25]. Additionally, Wang and Hebert (2016)[26] empirically show the existence of a generic nonlinear transformation from small-sample to large-sample models for different types of feature spaces and classifier models. Finally, Du et al. (2016)[27] provide theoretical guarantees on performance when one learns the transformation from the source function to a related target function. AlphaNet is similar in that we likewise infer that our target classifier is a transformation from a set of source classifiers.

2.4 Zero-shot/low-shot learning

Meta-learning, transfer learning, and learning-to-learn are frequently applied to the domain of low-shot learning[5,26,28–37]. A wide variety of prior studies have attempted to transfer knowledge from tasks with abundant data to completely novel tasks[8,25,38]. However, the explicit nature of low-shot learning consisting of tasks with small fixed samples means that these approaches do not generalize well beyond the arbitrary few tasks. This is a significant problem as the visual world clearly involves a wide set of tasks with continuously varying amounts of information.

2.5 Long-tailed learning

These restrictions on low-shot learning have directly led to the new paradigm referred to as long-tailed learning, where data samples are continuously decreasing and the data distribution closely models that of the visual world. Recent work achieves state-of-the-art performance on long-tailed recognition by learning multiple experts[39,40]. Both of these complex ensemble methods require a two-stage training method. A somewhat different approach re-balances the samples at different stages of model training[41], attempts to transfer features from common classes to rare classes[42], or transfers intra-class variance[43]. However, approaches to knowledge transfer require complex architectures, such as a specialized attention mechanism and memory models, as in the work of Liu et al. (2019)[42]. While most studies have largely focused on representation space transferability or complex ensembles, recent work establishes a strong baseline by exploring the potential of operating in classifier space[44]. Results suggest that decoupling model representation learning and classifier learning is a more efficient way to approach long-tailed learning. Specifically, methods normalizing classifiers and adjusting classifiers only using re-sampling strategies achieve good performance. Such successes in working only with classifiers support our general concept that combining strong classifiers in AlphaNet is a natural and direct way to improve upon weak classifiers.

3 Method

Given a long-tailed dataset, we will refer to the set of rare classes (which form the "tail" of the training data distribution) as the 'few' split, and the set of remaining classes as the 'base' split. AlphaNet is applied to update the 'few' split classifiers using nearest neighbors from the 'base' split.

Let C^F and C^B be the set of 'few' and 'base' split classes respectively. Following the notation described in Section 1.1, for a 'few' split class $c \in C^F$, let the k nearest 'base' split neighbors be $q_1^c, \ldots, q_k^c$. Let w^c be the classifier (a vector in $\mathbb{R}^d$) for c, and let $v_1^c, \ldots, v_k^c$ be the classifiers for its nearest neighbors.

3.1 Notation

We first group up our classes into two broad splits: our 'base' split with B number of classes and our 'few' split with F classes. The 'base' classes contain classes with many examples, and conversely the 'few' classes contain classes with few examples. We denote by $N = B + F$ the total number of classes.

Additionally, we denote a generic sample by I and its corresponding label by y. We split the training set into two subsets of pairs (I_i, y_i): the subset X_{base} contains samples from the B classes, and the subset X_{few} contains samples from the F classes.

Finally, we work with a fixed pre-trained model with classifiers W_j and biases b_j, $j \in (1, \ldots, N)$; here, classifiers are the last layers of networks, which map input representations to class scores. Given target class j, and its classifier W_j and bias b_j, let class j's top k nearest neighbor classifiers be defined as V_i^j , $i \in (1, \ldots, K)$. Furthermore, we also define the trivial case where the immediate nearest neighbor is itself, $V_0^j = W_j$.

3.2 AlphaNet

Our combination model, AlphaNet, takes in trained classifiers from the B 'base' classes and weak classifiers from the F 'few' classes, in order to learn a new classifier composition for each 'few' class. The following section will detail the model and our training as depicted in Figure 1.

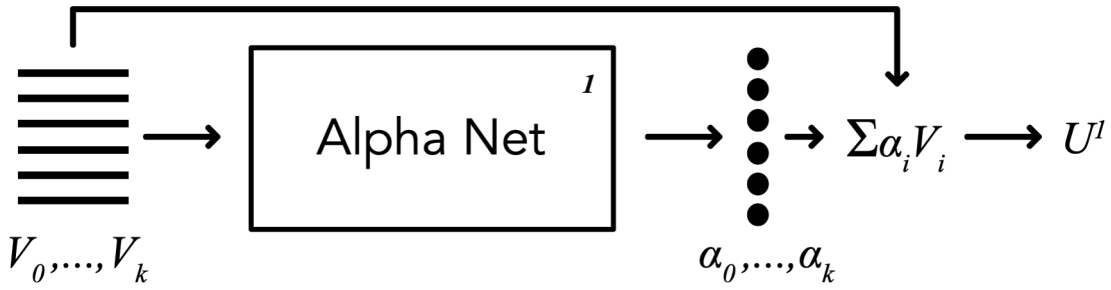

Figure 1: An illustration of AlphaNet. The classifier for a 'few' split class, along with the classifiers of k nearest neighbors are passed through a network, which outputs $k + 1$ weights, termed alphas. These alphas are used to linearly combine the input classifiers, producing the updated classifier for the given 'few' split class.

3.3 Architecture

AlphaNet is lightweight and uses a small fully connected network. Its input is a flattened concatenated vector of V_k^i, $k \in (0, \dots, K)$, where $V_0^i = W_i$, the original classifier for class i. Its output is an α vector, where α_k, $k \in (0, \dots, K)$ corresponds to input V_k^i. Importantly, AlphaNet does not restrict the range that α coefficients can be. Thus, AlphaNet learns both positive and negative α coefficients. Furthermore, AlphaNet can be used to learn all α coefficients for all classifiers. Once trained, AlphaNet can also be applied on new classes not seen during training.

3.4 Training

Given alphas α_k, and input V_k^i, $k \in (0, \dots, K)$, the updated classifier is given by

$$U_i = V_0 + \sum_{j=1}^{K} \alpha_j \cdot V_j^i. \tag{1}$$

We use the same set of alphas to learn U_i, $i \in (1, \dots, F)$ for each target class.

$$\begin{aligned} U_1 &= V_0^1 + \sum_{j=1}^{K} \alpha_j \cdot V_j^1. \\ U_F &= V_0^F \sum_{j=1}^{K} \alpha_j \cdot V_j^F. \end{aligned} \tag{2}$$

It is important to note that while we are attempting to compose new 'few' classifiers, we are still working on a long-tailed recognition problem. Thus, when training we must also consider our 'base' classifiers that have been sufficient trained. Now, given a training image sample and label pair $\{I_i, y_i\}$ and its final feature representation x_i, we compute our sample score as

$$\begin{aligned} s_{if} &= x_i \cdot U_f. \qquad f \in (1, \dots, F) \\ s_{ib} &= x_i \cdot W_b + b_b. \qquad b \in (1, \dots, B) \end{aligned} \tag{3}$$

We combine the two sets of scores and obtain per-class prediction scores. Finally, we compute the softmax cross entropy loss, which is minimized to learn AlphaNet weights.

4 Experiments

4.1 Experiment Setup

4.1.1 Datasets

We evaluated our method using three long-tailed benchmark datasets: ImageNet-LT, Places-LT [42], and CIFAR-100-LT
[45]. These Datasets are sampled from their respective original datasets, ImageNet [46], Places365 [47], and CIFAR-100 [48] such that the new distributions follow a standard long-tailed distribution.

ImageNet-LT contains 1000 classes with the number of samples per class ranging from 5 to 4980 images. Places-LT contains 365 classes with the number of samples per class ranging from 5 to 1280 images. CIFAR-100-LT contains 100 classes with the number of samples per class ranging from 5 to 500 images. For CIFAR-100-LT, we used the version described by Alshammari et al. (2022)[45], using an imbalance factor of 100.

The datasets are broken down into three broad splits that indicate the number of training samples per class: 1) 'many' contains classes with greater than 100 samples; 2) 'medium' contains classes with greater than or equal to 20 samples but less than or equal to 100 samples; 3) 'few' contains classes with less than 20 samples. The test set is always balanced, containing an equal number of samples for each class. We use the term 'base' split to refer to the combined 'many' and 'medium' splits.

Note: Another popular dataset used for testing long-tail learning models is iNaturalist[49]. Results for this dataset, however, are much more balanced across classes. So it does not represent a valid use case for our proposed method, and we omitted the dataset from our experiments.

4.1.2 Training data sampling

In order to prevent over-fitting on the 'few' split samples, we used a class balanced sampling approach, using all 'few' split samples, and a portion of the 'base' split samples. Given F 'few' split samples, and a ratio ρ, every epoch, ρF samples were drawn from the 'base' split, with sample weights inversely proportional to the class size. This ensured that all 'base' classes had an equal probability of being sampled. As we show in the following section, ρ allows us to control the balance between 'few' and 'base' split accuracy. We evaluated AlphaNet with a range of ρ values; results for $\rho = 0.5$, $\rho = 1$, and $\rho = 1.5$ are shown in Section 4.2, and the full set of results is in the appendix.

4.1.3 Training

All experiments used an AlphaNet module with three 32 unit layers, and Leaky-ReLU[?] activation. Unless stated otherwise, euclidean distance was used to find $k = 5$ nearest neighbors for each 'few' split class. Models were trained for 25 epochs to minimize cross-entropy loss computed using mini-batches of 64 samples. Optimization was performed using AdamW[50] with a learning rate of 0.001, decayed by a factor of 10, every 10 epochs. Model weights were saved after each epoch, and after training, the weights with the best accuracy on validation data were used to report results on the test set. All experiments were repeated 10 times, and we report mean and standard deviation of accuracies across trials.

4.2 Results

4.2.1 Baseline models

First, we applied AlphaNet on several strong baselines proposed by Kang et al. (2019)[44]. These methods have good overall accuracy, but accuracy for 'few' split classes is much lower. On the ImageNet-LT dataset, average accuracy for the cRT and LWS models (using a ResNeXt-50 backbone) is nearly 20 points below the overall accuracy, as seen in Table 1. Using features extracted from these two models, we used AlphaNet to update 'few' split classifiers. On both models, we saw a significant increase in the 'few' split accuracy for all values of ρ, leading to more balanced accuracies.

For $\rho = 1$, average 'few' split accuracy was boosted by 7 points for the cRT model, and about 11 points for the LWS model, while overall accuracy was within 2 point of the original. We found this value of ρ to provide a good balance between 'few' split and overall accuracy. Lower values of ρ led to much larger 'few' split accuracy, and even with $\rho = 1.5$, there was a significant increase, while the accuracy for other splits remained around the same.

Method	Few	Med.	Many	Overall
Cross entropy†	7.7	37.5	65.9	44.4
NCM†	28.1	45.3	56.6	47.3
τ-normalized†	30.7	46.9	59.1	49.4
cRT†	27.4	46.2	61.8	49.6
Alpha-cRT ($\rho = 0.5$)	$39.7^{\pm 1.42}$	$42.0^{\pm 0.66}$	$58.3^{\pm 0.52}$	$48.0^{\pm 0.37}$
Alpha-cRT ($\rho = 1$)	$34.6^{\pm 1.88}$	$43.7^{\pm 0.51}$	$59.7^{\pm 0.43}$	$48.6^{\pm 0.24}$
Alpha-cRT ($\rho = 1.5$)	$32.6^{\pm 2.46}$	$44.4^{\pm 0.49}$	$60.3^{\pm 0.38}$	$48.9^{\pm 0.19}$
LWS†	30.4	47.2	60.2	49.9
Alpha-LWS ($\rho = 0.5$)	$46.9^{\pm 0.98}$	$38.6^{\pm 0.87}$	$52.9^{\pm 0.86}$	$45.3^{\pm 0.69}$
Alpha-LWS ($\rho = 1$)	$41.6^{\pm 1.61}$	$42.2^{\pm 0.53}$	$56.0^{\pm 0.32}$	$47.4^{\pm 0.30}$
Alpha-LWS ($\rho = 1.5$)	$40.1^{\pm 1.99}$	$43.2^{\pm 0.98}$	$56.9^{\pm 0.76}$	$48.0^{\pm 0.53}$

Table 1: Baseline methods on ImageNet-LT. † indicates results that were taken directly from Kang et al. (2019)[44]. Alpha-cRT, and Alpha-LWS are AlphaNet models applied over cRT and LWS features respectively.

We repeated the above experiment on the Places-LT dataset, where again 'few' split accuracy for the cRT and LWS models is much lower than the overall accuracy (by around 12 and 9 points respectively as seen in Table 2. With $\rho = 1$, AlphaNet improved 'few' split accuracy by 2 points on average for the cRT model, and about 6 points on average for the LWS model. In both cases, overall accuracy was within 1 point of the baseline.

4.2.2 State-of-the-art

Next, we applied AlphaNet on two state-of-the-art models. First, we used the 6-expert teacher model of Wang et al. (2020)[40]. We provided the combined feature vectors from all 6 experts as input to AlphaNet. The learned 'few' split classifiers were split into 6, and used to update the experts. Prediction scores from the experts were averaged to produce the final predictions, as in the original model. For ImageNet-LT, the experts used a ResNeXt-50 backbone, and for CIFAR-100-LT, a ResNet-32 backbone. Table 3 shows the base results for the expert models, along with AlphaNet results for $\rho = 0.5, 1, 2$. On ImageNet-LT, 'few' split accuracy was increased by up to 7 points, and on CIFAR-100-LT, by 5 points. The second state-of-the-art model we used was the weight balancing method proposed by Alshammari et al. (2022)[45]. The full set of results on the CIFAR-100-LT dataset is shown in the appendix.

Method	Few	Med.	Many	Overall
Cross entropy†	8.2	27.3	45.7	30.2
NCM†	27.3	37.1	40.4	36.4
τ-normalized†	31.8	40.7	37.8	37.9
cRT	24.9	37.6	42.0	36.7
Alpha-cRT ($\rho = 0.5$)	$31.0^{\pm 0.88}$	$34.5^{\pm 0.17}$	$40.4^{\pm 0.29}$	$35.9^{\pm 0.09}$
Alpha-cRT ($\rho = 1$)	$27.0^{\pm 1.02}$	$36.1^{\pm 0.31}$	$41.3^{\pm 0.13}$	$36.2^{\pm 0.10}$
Alpha-cRT ($\rho = 1.5$)	$25.5^{\pm 0.89}$	$36.5^{\pm 0.36}$	$41.6^{\pm 0.21}$	$36.2^{\pm 0.11}$
LWS	28.7	39.1	40.6	37.6
Alpha-LWS ($\rho = 0.5$)	$37.1^{\pm 1.39}$	$34.4^{\pm 0.80}$	$37.7^{\pm 0.52}$	$36.1^{\pm 0.31}$
Alpha-LWS ($\rho = 1$)	$34.6^{\pm 0.97}$	$35.8^{\pm 0.54}$	$38.6^{\pm 0.39}$	$36.6^{\pm 0.22}$
Alpha-LWS ($\rho = 1.5$)	$32.2^{\pm 1.17}$	$37.2^{\pm 0.36}$	$39.5^{\pm 0.39}$	$37.0^{\pm 0.11}$

Table 2: Baseline methods on Places-LT. † indicates results that were taken directly from Kang et al. (2019) [44]. Alpha-cRT, and Alpha-LWS are AlphaNet models applied over cRT and LWS features respectively.

Method	Few	Med.	Many	Overall
ImageNet-LT				
RIDE	36.5	54.4	68.9	57.5
Alpha-RIDE ($\rho = 0.5$)	$43.5^{\pm 0.75}$	$52.3^{\pm 0.26}$	$67.3^{\pm 0.17}$	$56.9^{\pm 0.11}$
Alpha-RIDE ($\rho = 1$)	$40.8^{\pm 1.00}$	$53.1^{\pm 0.21}$	$67.9^{\pm 0.18}$	$57.1^{\pm 0.11}$
Alpha-RIDE ($\rho = 1.5$)	$38.2^{\pm 1.22}$	$53.6^{\pm 0.25}$	$68.4^{\pm 0.17}$	$57.2^{\pm 0.06}$
CIFAR-100-LT				
RIDE	25.8	52.1	69.3	50.2
Alpha-RIDE ($\rho = 0.5$)	$30.9^{\pm 1.82}$	$47.0^{\pm 1.25}$	$65.7^{\pm 0.94}$	$48.7^{\pm 0.41}$
Alpha-RIDE ($\rho = 1$)	$27.2^{\pm 1.69}$	$49.1^{\pm 0.85}$	$67.4^{\pm 0.62}$	$48.9^{\pm 0.30}$
Alpha-RIDE ($\rho = 1.5$)	$25.0^{\pm 1.15}$	$50.1^{\pm 1.12}$	$67.9^{\pm 1.01}$	$48.8^{\pm 0.63}$

Table 3: ImageNet-LT and CIFAR-100-LT results using the ensemble model proposed by Wang et al. (2020) [40]. Alpha-RIDE applies AlphaNet on average features from the ensemble.

4.2.3 Comparison with control

Our method is based on the core hypothesis that classifiers can be improved using nearest neighbors. In this section, we directly test this hypothesis. Based on the results in the previous section, the improvements in 'few' split accuracy could be attributed simply to the extra fine-tuning of 'few' split classifiers. So, we repeated the experiments of the previous section with randomly chosen neighbors for each 'few' split class, rather than nearest neighbors. This differs from our previous experiments only in the nature of neighbors used, so if our method's improvements are solely due

to extra fine-tuning, we should see the same results. However, as seen in Figure 2, training with nearest neighbors garners much larger improvements in 'few' split accuracy, with similar trends in overall accuracy. This supports our hypothesis that data-poor classes can make use of data from neighbors to improve classification performance.

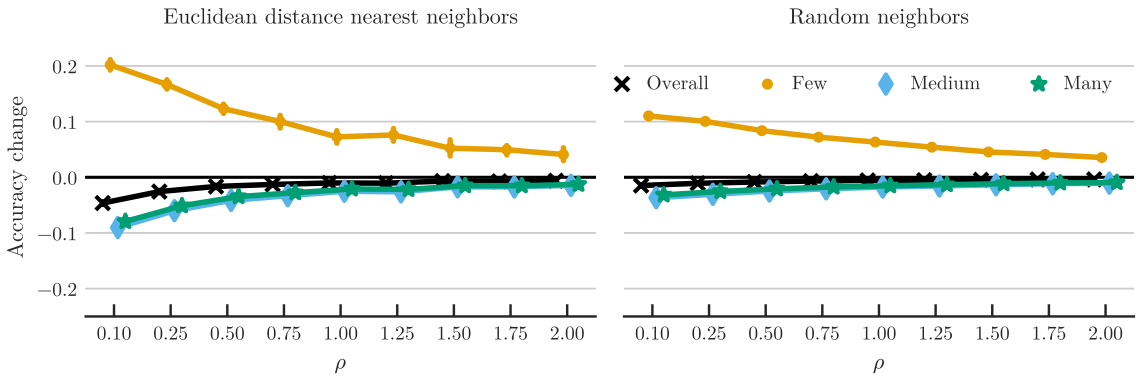

Figure 2: Change in split accuracy for AlphaNet training of cRT model on ImageNet-LT. For each value of ρ, the two plots both show the change in split accuracy for AlphaNet compared to the baseline cRT model, as well as the change in overall accuracy. Plot a) shows the results for normal training with 5 euclidean nearest neighbors, and plot b) shows the results for training with 5 random neighbors for each 'few' split class. Training with nearest neighbors leads to much larger increase in 'few' split accuracy (especially for small values of ρ), which cannot be accounted for by the additional fine-tuning of classifiers.

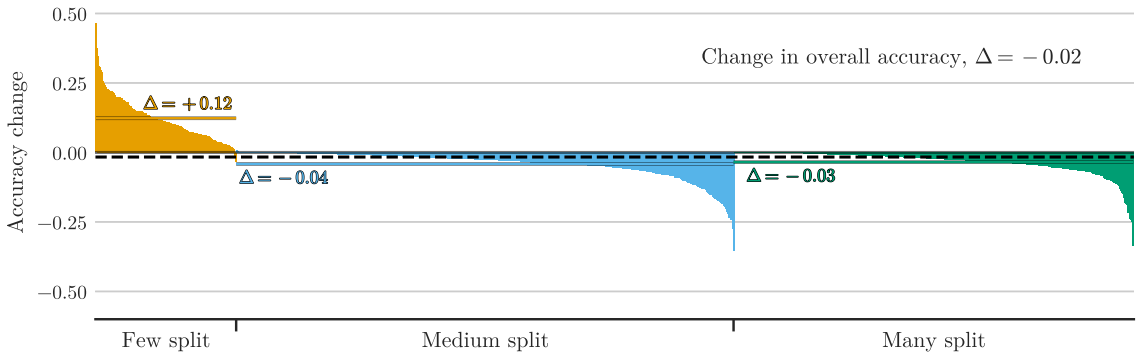

Figure 3: Change in per-class test accuracy for AlphaNet applied over cRT features, with $\rho = 0.5$. Within each split, the classes are sorted by change in accuracy, and the dashed line shows the average per-class change (change value Δ). The spanning dashed line shows the mean overall change in per-class test accuracy. Nearly all 'few' split classes have their accuracy improved, and the overall improvement of 'few' split accuracy far exceeds the average decrease for 'many' and 'medium' splits.

...

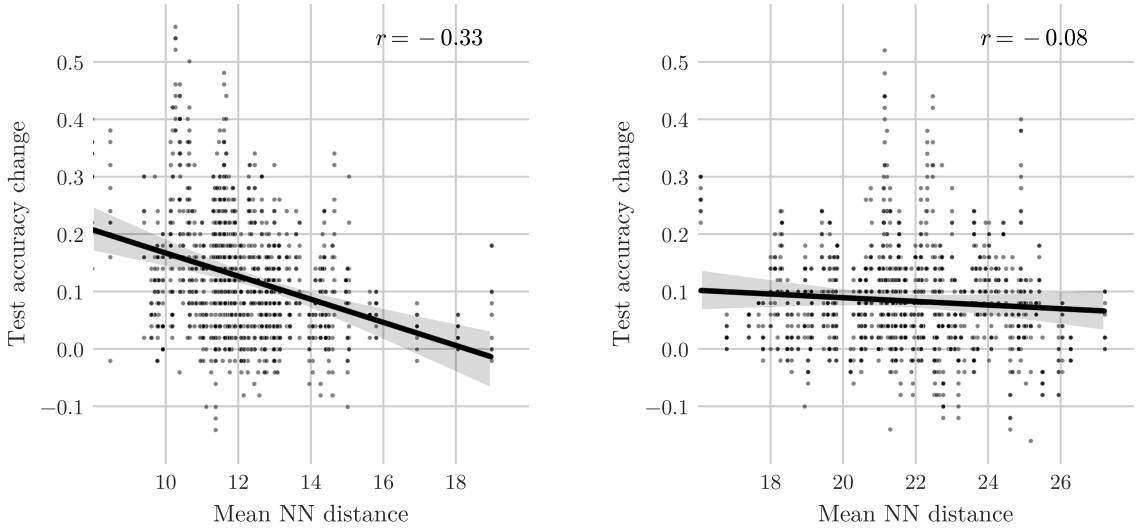

(a) Five nearest neighbors by Euclidean distance

(b) Five random neighbors

Figure 4: Change in per-class accuracy for AlphaNet applied over cRT features, with $\rho = 0.5$, versus mean Euclidean distance to five neighbors. Figure 4a uses five nearest neighbors by Euclidean neighbors, and Figure 4b uses five random neighbors. Both plots show results from ten runs with random starts. Comparing with Figure **??**, we can see that AlphaNet provides the largest boost to classes with poor baseline performance, which have close nearest neighbors.

...

...

5 Conclusion

The long-tailed nature of the world presents a challenge for any model that depends on learning over specific examples. Most long-tailed methods tend to have high overall accuracy, but with unbalanced accuracies where frequent classes are learned well with high accuracies and rare classes are learned poorly with low accuracies. As such, the long-tailed world represents one source of potential bias [along with the models themselves and system designer decisions; Lara et al. (2022)[51]]. To address this problem, typical approaches resort to re-sampling or re-weighting of rare classes but still focus on achieving the highest overall accuracy. Consequently, these methods continue to suffer from an accuracy imbalance across data-rich and data-poor classes. In contrast, our method, AlphaNet, provides a rapid 5 minute *post-hoc* correction that can sit on top of any model using classifiers. This simple method re-balances classification accuracy quickly so that rare classes have much higher accuracy, but overall classification accuracy is preserved. In addition to directly addressing training imbalances, AlphaNet is also applicable to re-balancing accuracies across biases arising from model structure or the prioritization of different model parameters. That is, AlphaNet is deployable in any

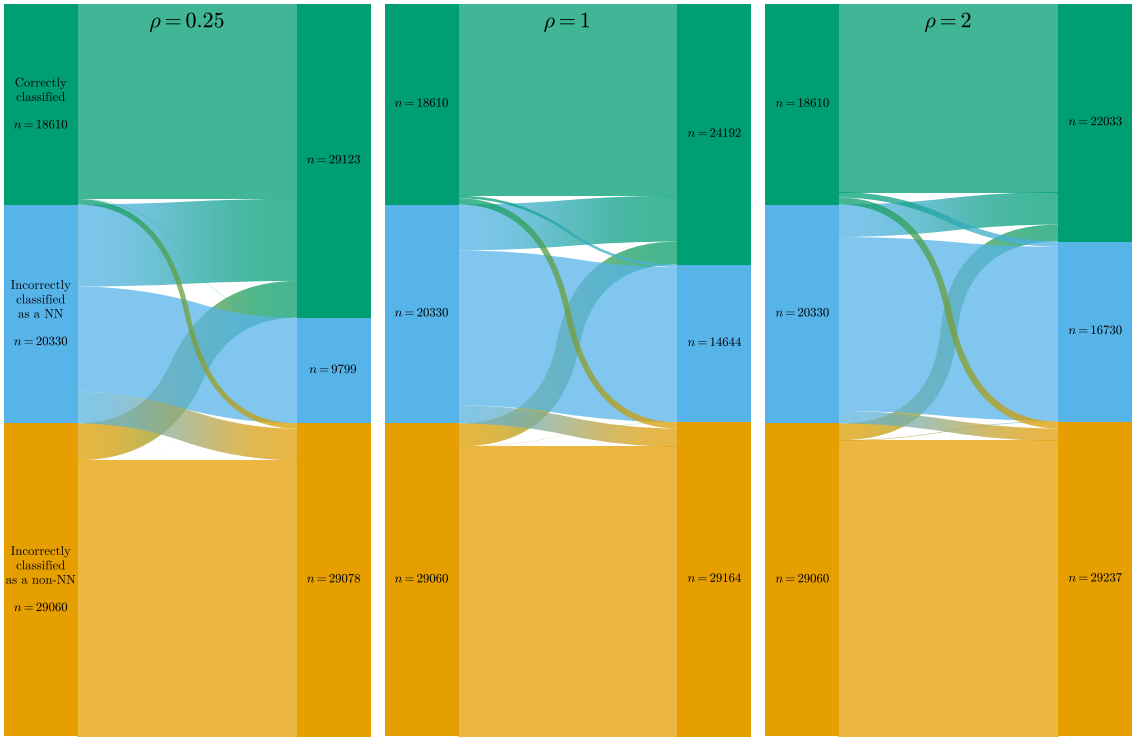

Figure 5: Change in 'few' split sample predictions for AlphaNet applied for cRT features, with $k = 10$ nearest neighbors by Euclidean distance. In each chart, the bars on the left show the distribution of predictions for 'few' split test samples, by the baseline model; and the bars on the right show the distribution for AlphaNet. The predictions are grouped into three categories: 1) correct predictions, 2) incorrect predictions where the prediction was a nearest neighbor of the original class (e.g., predicting 'Malamute' for 'Husky'), and 3) all other incorrect predictions. The "flow" bands from left to right show the changes in individual sample predictions. There is a large improvement for samples previously misclassified as a nearest neighbor, particularly for small ρ. As ρ is increased, smaller portion of these mistakes are corrected, leading to smaller improvement in 'few' split accuracy.

application where the base classifiers cannot be changed, but balanced performance is desirable – thereby making it useful in contexts where ethics, privacy, or intellectual property are concerns.

References

[1] Sebastian Thrun. Learning to learn. pages 181–209, 1998. doi: 10.1007/978-1-4615-5529-2_8.

[2] Jürgen Schmidhuber, Jieyu Zhao, and Marco Wiering. Shifting inductive bias with success-story

algorithm, adaptive levin search, and incremental self-improvement. *Machine Learning*, 28(1): 105–130, 1997. ISSN 0885-6125. doi: 10.1023/a:1007383707642.

[3] Sinno Jialin Pan and Qiang Yang. A survey on transfer learning. *IEEE Transactions on Knowledge and Data Engineering*, 22(10):1345–1359, 2009. ISSN 1041-4347. doi: 10.1109/tkde.2009.191.

[4] Rich Caruana. Multitask learning. *Machine Learning*, 28(1):41–75, 1997. ISSN 0885-6125. doi: 10.1023/a:1007379606734.

[5] Adam Santoro, Sergey Bartunov, Matthew Botvinick, Daan Wierstra, and Timothy Lillicrap. One-shot learning with memory-augmented neural networks. *arXiv*, 2016. doi: 10.48550/arxiv.1605.06065.

[6] J. Schmidhuber. A neural network that embeds its own meta-levels. *IEEE International Conference on Neural Networks*, pages 407–412 vol.1, 1993. doi: 10.1109/icnn.1993.298591.

[7] Jrgen Schmidhuber. Learning to control fast-weight memories: An alternative to dynamic recurrent networks. *Neural Computation*, 4(1):131–139, 1992. ISSN 0899-7667. doi: 10.1162/neco.1992.4.1.131.

[8] Luca Bertinetto, João F Henriques, Jack Valmadre, Philip H S Torr, and Andrea Vedaldi. Learning feed-forward one-shot learners. *arXiv*, 2016. doi: 10.48550/arxiv.1606.05233.

[9] David Ha, Andrew Dai, and Quoc V Le. Hypernetworks. *arXiv*, 2016. doi: 10.48550/arxiv.1609.09106.

[10] Chelsea Finn, Kelvin Xu, and Sergey Levine. Probabilistic model-agnostic meta-learning. *arXiv*, 2018. doi: 10.48550/arxiv.1806.02817.

[11] Sylvestre-Alvise Rebuffi, Hakan Bilen, and Andrea Vedaldi. Learning multiple visual domains with residual adapters. *arXiv*, 2017. doi: 10.48550/arxiv.1705.08045.

[12] Abhishek Sinha, Mausoom Sarkar, Aahitagni Mukherjee, and Balaji Krishnamurthy. Introspection: Accelerating neural network training by learning weight evolution. *arXiv*, 2017. doi: 10.48550/arxiv.1704.04959.

[13] Tsendsuren Munkhdalai and Hong Yu. Meta networks. *Proceedings of machine learning research*, 70:2554–2563, 2017.

[14] Richard Socher, Milind Ganjoo, Hamsa Sridhar, Osbert Bastani, Christopher D Manning, and Andrew Y Ng. Zero-shot learning through cross-modal transfer. *arXiv*, 2013. doi: 10.48550/arxiv.1301.3666.

[15] Jimmy Lei Ba, Kevin Swersky, Sanja Fidler, and Ruslan Salakhutdinov. Predicting deep zero-shot convolutional neural networks using textual descriptions. *2015 IEEE International Conference on Computer Vision (ICCV)*, pages 4247–4255, 2015. doi: 10.1109/iccv.2015.483.

[16] Hyeonwoo Noh, Paul Hongsuck Seo, and Bohyung Han. Image question answering using convolutional neural network with dynamic parameter prediction. *2016 IEEE Conference on Computer Vision and Pattern Recognition (CVPR)*, pages 30–38, 2016. doi: 10.1109/cvpr.2016.11.

[17] Jason Weston, Samy Bengio, and Nicolas Usunier. Large scale image annotation: learning to rank with joint word-image embeddings. *Machine Learning*, 81(1):21–35, 2010. ISSN 0885-6125. doi: 10.1007/s10994-010-5198-3.

[18] Gang Wang, Derek Hoiem, and David Forsyth. Learning image similarity from flickr groups using fast kernel machines. *IEEE Transactions on Pattern Analysis and Machine Intelligence*, 34(11):2177–2188, 2012. ISSN 0162-8828. doi: 10.1109/tpami.2012.29.

[19] Ioannis Tsochantaridis, Thorsten Joachims, Thomas Hofmann, Yasemin Altun, and Yoram Singer. Large margin methods for structured and interdependent output variables. *Journal of machine learning research*, 6(9), 2005.

[20] Yusuf Aytar and Andrew Zisserman. Enhancing exemplar svms using part level transfer regularization. *Procedings of the British Machine Vision Conference 2012*, pages 79.1–79.11, 2012. doi: 10.5244/c.26.79.

[21] Mohamed Elhoseiny, Babak Saleh, and Ahmed Elgammal. Write a classifier: Zero-shot learning using purely textual descriptions. *2013 IEEE International Conference on Computer Vision*, pages 2584–2591, 2013. doi: 10.1109/iccv.2013.321.

[22] Ishan Misra, Abhinav Gupta, and Martial Hebert. From red wine to red tomato: Composition with context. *2017 IEEE Conference on Computer Vision and Pattern Recognition (CVPR)*, pages 1160–1169, 2017. doi: 10.1109/cvpr.2017.129.

[23] Soravit Changpinyo, Wei-Lun Chao, Boqing Gong, and Fei Sha. Synthesized classifiers for zero-shot learning. *2016 IEEE Conference on Computer Vision and Pattern Recognition (CVPR)*, pages 5327–5336, 2016. doi: 10.1109/cvpr.2016.575.

[24] Marcin Andrychowicz, Misha Denil, Sergio Gomez, Matthew W Hoffman, David Pfau, Tom Schaul, Brendan Shillingford, and Nando de Freitas. Learning to learn by gradient descent by gradient descent. *arXiv*, 2016. doi: 10.48550/arxiv.1606.04474.

[25] Sachin Ravi and Hugo Larochelle. Optimization as a model for few-shot learning. 2016.

[26] Yu-Xiong Wang and Martial Hebert. Computer vision – eccv 2016, 14th european conference, amsterdam, the netherlands, october 11-14, 2016, proceedings, part vi. *Lecture Notes in Computer Science*, pages 616–634, 2016. ISSN 0302-9743. doi: 10.1007/978-3-319-46466-4_37.

[27] Simon Shaolei Du, Jayanth Koushik, Aarti Singh, and Barnabas Poczos. Hypothesis transfer learning via transformation functions. *arXiv*, 2016. doi: 10.48550/arxiv.1612.01020.

[28] Li Fei-Fei, Rob Fergus, and Pietro Perona. One-shot learning of object categories. *IEEE Transactions on Pattern Analysis and Machine Intelligence*, 28(4):594–611, 2006. ISSN 0162-8828. doi: 10.1109/tpami.2006.79.

[29] Gregory Koch, Richard Zemel, and Ruslan Salakhutdinov. Siamese neural networks for one-shot image recognition. In *ICML deep learning workshop*, volume 2, page 0.

[30] Brenden M. Lake, Ruslan Salakhutdinov, and Joshua B. Tenenbaum. Human-level concept learning through probabilistic program induction. *Science*, 350(6266):1332–1338, 2015. ISSN 0036-8075. doi: 10.1126/science.aab3050.

[31] Zhizhong Li and Derek Hoiem. Learning without forgetting. *arXiv*, 2016. doi: 10.48550/arxiv.1606.09282.

[32] Bharath Hariharan and Ross Girshick. Low-shot visual recognition by shrinking and hallucinating features. *2017 IEEE International Conference on Computer Vision (ICCV)*, pages 3037–3046, 2017. doi: 10.1109/iccv.2017.328.

[33] JANE BROMLEY, JAMES W BENTZ, LÉON BOTTOU, ISABELLE GUYON, YANN LECUN, CLIFF MOORE, EDUARD SÄCKINGER, and ROOPAK SHAH. Signature verification using a "siamese" time delay neural network. *International Journal of Pattern Recognition and Artificial Intelligence*, 07(04):669–688, 1993. ISSN 0218-0014. doi: 10.1142/s0218001493000339.

[34] Jake Snell, Kevin Swersky, and Richard S Zemel. Prototypical networks for few-shot learning. *arXiv*, 2017. doi: 10.48550/arxiv.1703.05175.

[35] Dileep George, Wolfgang Lehrach, Ken Kansky, Miguel Lázaro-Gredilla, Christopher Laan, Bhaskara Marthi, Xinghua Lou, Zhaoshi Meng, Yi Liu, Huayan Wang, Alex Lavin, and D. Scott Phoenix. A generative vision model that trains with high data efficiency and breaks text-based captchas. *Science*, 358(6368), 2017. ISSN 0036-8075. doi: 10.1126/science.aag2612.

[36] Yu-Xiong Wang, Deva Ramanan, and Martial Hebert. Learning to model the tail. *Advances in neural information processing systems*, 30, 2017.

[37] Zeynep Akata, Florent Perronnin, Zaid Harchaoui, and Cordelia Schmid. Label-embedding for image classification. *IEEE Transactions on Pattern Analysis and Machine Intelligence*, 38(7): 1425–1438, 2015. ISSN 0162-8828. doi: 10.1109/tpami.2015.2487986.

[38] Oriol Vinyals, Charles Blundell, Timothy Lillicrap, Koray Kavukcuoglu, and Daan Wierstra. Matching networks for one shot learning. *arXiv*, 2016. doi: 10.48550/arxiv.1606.04080.

[39] Jiarui Cai, Yizhou Wang, and Jenq-Neng Hwang. Ace: Ally complementary experts for solving long-tailed recognition in one-shot. *2021 IEEE/CVF International Conference on Computer Vision (ICCV)*, 00:112–121, 2021. doi: 10.1109/iccv48922.2021.00018.

[40] Xudong Wang, Long Lian, Zhongqi Miao, Ziwei Liu, and Stella X Yu. Long-tailed recognition by routing diverse distribution-aware experts. *arXiv*, 2020. doi: 10.48550/arxiv.2010.01809.

[41] Kaidi Cao, Colin Wei, Adrien Gaidon, Nikos Arechiga, and Tengyu Ma. Learning imbalanced datasets with label-distribution-aware margin loss. *arXiv*, 2019. doi: 10.48550/arxiv.1906.07413.

[42] Ziwei Liu, Zhongqi Miao, Xiaohang Zhan, Jiayun Wang, Boqing Gong, and Stella X. Yu. Large-scale long-tailed recognition in an open world. *2019 IEEE/CVF Conference on Computer Vision and Pattern Recognition (CVPR)*, 00:2532–2541, 2019. doi: 10.1109/cvpr.2019.00264.

[43] Xi Yin, Xiang Yu, Kihyuk Sohn, Xiaoming Liu, and Manmohan Chandraker. Feature transfer learning for face recognition with under-represented data. *2019 IEEE/CVF Conference on Computer Vision and Pattern Recognition (CVPR)*, 00:5697–5706, 2019. doi: 10.1109/cvpr.2019.00585.

[44] Bingyi Kang, Saining Xie, Marcus Rohrbach, Zhicheng Yan, Albert Gordo, Jiashi Feng, and Yannis Kalantidis. Decoupling representation and classifier for long-tailed recognition. *arXiv*, 2019.

[45] Shaden Alshammari, Yu-Xiong Wang, Deva Ramanan, and Shu Kong. Long- tailed recognition via weight balancing. *2022 IEEE/CVF Conference on Computer Vision and Pattern Recognition (CVPR)*, 00:6887–6897, 2022. doi: 10.1109/cvpr52688.2022.00677.

[46] Olga Russakovsky, Jia Deng, Hao Su, Jonathan Krause, Sanjeev Satheesh, Sean Ma, Zhiheng Huang, Andrej Karpathy, Aditya Khosla, Michael Bernstein, Alexander C. Berg, and Li Fei-Fei. Imagenet large scale visual recognition challenge. *International Journal of Computer Vision*, 115(3):211–252, 2015. ISSN 0920-5691. doi: 10.1007/s11263-015-0816-y.

[47] Bolei Zhou, Agata Lapedriza, Aditya Khosla, Aude Oliva, and Antonio Torralba. Places: A 10 million image database for scene recognition. *IEEE Transactions on Pattern Analysis and Machine Intelligence*, 40(6):1452–1464, 2017. ISSN 0162-8828. doi: 10.1109/tpami.2017.2723009.

[48] Alex Krizhevsky and Geoffrey Hinton. Learning multiple layers of features from tiny images. 2009.

[49] Grant Van Horn, Oisin Mac Aodha, Yang Song, Yin Cui, Chen Sun, Alex Shepard, Hartwig Adam, Pietro Perona, and Serge Belongie. The inaturalist species classification and detection dataset. *2018 IEEE/CVF Conference on Computer Vision and Pattern Recognition*, pages 8769–8778, 2018. doi: 10.1109/cvpr.2018.00914.

[50] Ilya Loshchilov and Frank Hutter. Decoupled weight decay regularization. *arXiv*, 2017. doi: 10.48550/arxiv.1711.05101.

[51] María Agustina Ricci Lara, Rodrigo Echeveste, and Enzo Ferrante. Addressing fairness in artificial intelligence for medical imaging. *Nature Communications*, 13(1):4581, 2022. doi: 10.1038/s41467-022-32186-3.

A1 Appendix

A1.1 ImageNet-LT Results

Experiment	Few	Med.	Many	Overall
Baseline	27.4	46.2	61.8	49.6
AlphaNet ($\rho = 0.1$)	$47.6^{\pm 1.60}$	$37.1^{\pm 0.76}$	$53.8^{\pm 0.62}$	$45.0^{\pm 0.41}$
AlphaNet ($\rho = 0.2$)	$45.7^{\pm 1.56}$	$39.0^{\pm 0.78}$	$55.7^{\pm 0.79}$	$46.3^{\pm 0.52}$
AlphaNet ($\rho = 0.25$)	$44.1^{\pm 1.44}$	$40.2^{\pm 0.65}$	$56.7^{\pm 0.57}$	$47.1^{\pm 0.36}$
AlphaNet ($\rho = 0.3$)	$42.9^{\pm 1.29}$	$40.4^{\pm 0.72}$	$57.0^{\pm 0.68}$	$47.1^{\pm 0.47}$
AlphaNet ($\rho = 0.4$)	$40.8^{\pm 1.85}$	$41.5^{\pm 0.72}$	$57.8^{\pm 0.54}$	$47.7^{\pm 0.36}$
AlphaNet ($\rho = 0.5$)	$39.7^{\pm 1.42}$	$42.0^{\pm 0.66}$	$58.3^{\pm 0.52}$	$48.0^{\pm 0.37}$
AlphaNet ($\rho = 0.75$)	$37.4^{\pm 1.93}$	$42.9^{\pm 0.46}$	$59.0^{\pm 0.40}$	$48.3^{\pm 0.16}$
AlphaNet ($\rho = 1$)	$34.6^{\pm 1.88}$	$43.7^{\pm 0.51}$	$59.7^{\pm 0.43}$	$48.6^{\pm 0.24}$
AlphaNet ($\rho = 1.25$)	$35.0^{\pm 1.98}$	$43.6^{\pm 0.70}$	$59.6^{\pm 0.50}$	$48.6^{\pm 0.35}$
AlphaNet ($\rho = 1.5$)	$32.6^{\pm 2.46}$	$44.4^{\pm 0.49}$	$60.3^{\pm 0.38}$	$48.9^{\pm 0.19}$
AlphaNet ($\rho = 1.75$)	$32.3^{\pm 1.42}$	$44.4^{\pm 0.32}$	$60.3^{\pm 0.18}$	$48.9^{\pm 0.14}$
AlphaNet ($\rho = 2$)	$31.5^{\pm 1.99}$	$44.7^{\pm 0.46}$	$60.5^{\pm 0.30}$	$49.0^{\pm 0.12}$
AlphaNet ($\rho = 3$)	$29.0^{\pm 2.05}$	$45.1^{\pm 0.36}$	$60.9^{\pm 0.28}$	$49.0^{\pm 0.08}$

Table A1: AlphaNet with cRT baseline on ImageNet-LT.

Experiment	Few	Med.	Many	Overall
Baseline	30.4	47.2	60.2	49.9
AlphaNet ($\rho = 0.1$)	$53.9^{\pm 0.77}$	$29.4^{\pm 1.22}$	$44.2^{\pm 1.22}$	$38.5^{\pm 1.03}$
AlphaNet ($\rho = 0.2$)	$52.0^{\pm 1.21}$	$33.3^{\pm 1.44}$	$48.0^{\pm 1.37}$	$41.5^{\pm 1.08}$
AlphaNet ($\rho = 0.25$)	$51.1^{\pm 0.63}$	$34.4^{\pm 1.04}$	$48.9^{\pm 0.99}$	$42.3^{\pm 0.82}$
AlphaNet ($\rho = 0.3$)	$49.8^{\pm 2.20}$	$35.9^{\pm 1.59}$	$50.4^{\pm 1.47}$	$43.4^{\pm 1.10}$
AlphaNet ($\rho = 0.4$)	$48.7^{\pm 1.17}$	$37.4^{\pm 1.13}$	$51.6^{\pm 0.95}$	$44.4^{\pm 0.80}$
AlphaNet ($\rho = 0.5$)	$46.9^{\pm 0.98}$	$38.6^{\pm 0.87}$	$52.9^{\pm 0.86}$	$45.3^{\pm 0.69}$
AlphaNet ($\rho = 0.75$)	$45.3^{\pm 1.89}$	$40.2^{\pm 1.28}$	$54.4^{\pm 1.01}$	$46.3^{\pm 0.76}$
AlphaNet ($\rho = 1$)	$41.6^{\pm 1.61}$	$42.2^{\pm 0.53}$	$56.0^{\pm 0.32}$	$47.4^{\pm 0.30}$
AlphaNet ($\rho = 1.25$)	$42.5^{\pm 1.41}$	$42.1^{\pm 0.74}$	$56.0^{\pm 0.53}$	$47.5^{\pm 0.41}$
AlphaNet ($\rho = 1.5$)	$40.1^{\pm 1.99}$	$43.2^{\pm 0.98}$	$56.9^{\pm 0.76}$	$48.0^{\pm 0.53}$
AlphaNet ($\rho = 1.75$)	$39.4^{\pm 2.53}$	$43.5^{\pm 0.88}$	$57.1^{\pm 0.70}$	$48.2^{\pm 0.45}$
AlphaNet ($\rho = 2$)	$37.5^{\pm 2.94}$	$44.3^{\pm 0.86}$	$57.9^{\pm 0.72}$	$48.6^{\pm 0.32}$
AlphaNet ($\rho = 3$)	$34.5^{\pm 1.91}$	$45.3^{\pm 0.54}$	$58.7^{\pm 0.37}$	$49.0^{\pm 0.21}$

Table A2: AlphaNet with LWS baseline on ImageNet-LT.

A1.2 Places-LT Results

A1.3 CIFAR100-LT Results

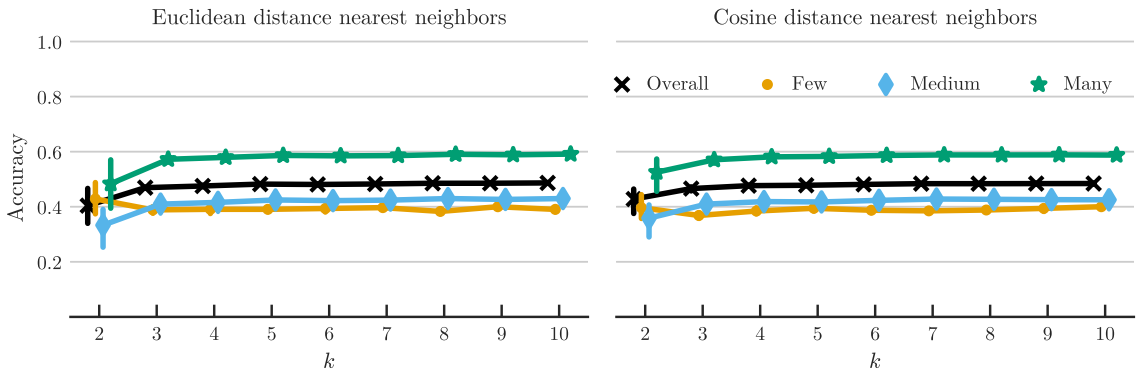

Figure A1: ...

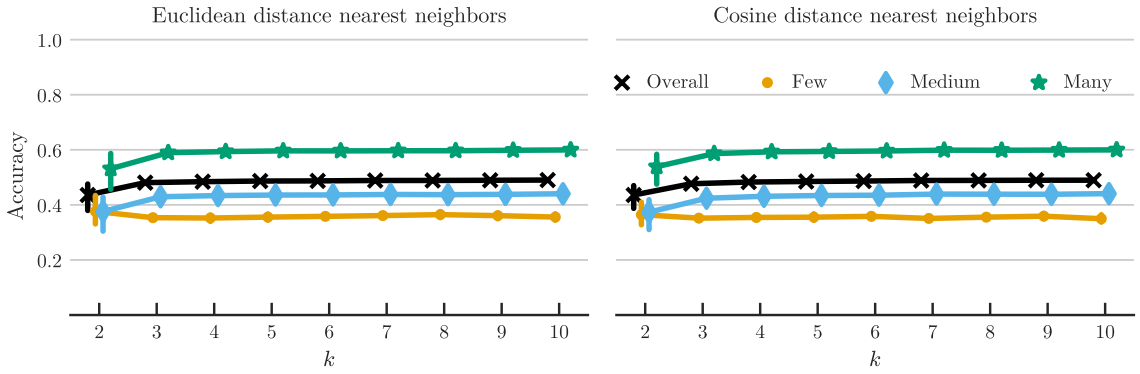

Figure A2: ...

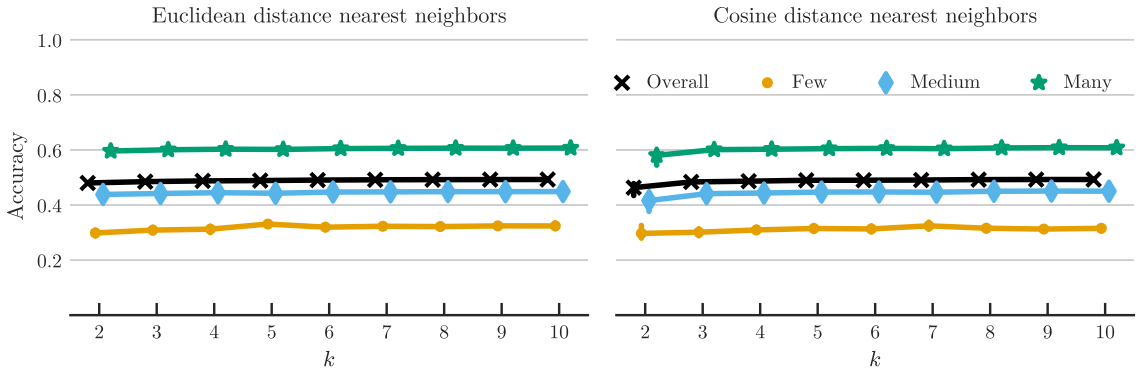

Figure A3: ...

Experiment	Few	Med.	Many	Overall
Baseline	36.5	54.4	68.9	57.5
AlphaNet ($\rho = 0.1$)	$49.2^{\pm 0.69}$	$49.5^{\pm 0.40}$	$65.4^{\pm 0.16}$	$55.6^{\pm 0.19}$
AlphaNet ($\rho = 0.2$)	$47.1^{\pm 0.86}$	$50.5^{\pm 0.34}$	$66.0^{\pm 0.20}$	$56.0^{\pm 0.16}$
AlphaNet ($\rho = 0.25$)	$46.8^{\pm 0.59}$	$50.7^{\pm 0.29}$	$66.2^{\pm 0.25}$	$56.2^{\pm 0.23}$
AlphaNet ($\rho = 0.3$)	$46.1^{\pm 1.16}$	$51.2^{\pm 0.50}$	$66.5^{\pm 0.29}$	$56.4^{\pm 0.21}$
AlphaNet ($\rho = 0.4$)	$44.7^{\pm 1.13}$	$51.7^{\pm 0.39}$	$66.9^{\pm 0.24}$	$56.6^{\pm 0.22}$
AlphaNet ($\rho = 0.5$)	$43.5^{\pm 0.75}$	$52.3^{\pm 0.26}$	$67.3^{\pm 0.17}$	$56.9^{\pm 0.11}$
AlphaNet ($\rho = 0.75$)	$41.7^{\pm 0.63}$	$52.8^{\pm 0.18}$	$67.7^{\pm 0.15}$	$57.0^{\pm 0.12}$
AlphaNet ($\rho = 1$)	$40.8^{\pm 1.00}$	$53.1^{\pm 0.21}$	$67.9^{\pm 0.18}$	$57.1^{\pm 0.11}$
AlphaNet ($\rho = 1.25$)	$39.0^{\pm 1.28}$	$53.4^{\pm 0.22}$	$68.2^{\pm 0.16}$	$57.2^{\pm 0.05}$
AlphaNet ($\rho = 1.5$)	$38.2^{\pm 1.22}$	$53.6^{\pm 0.25}$	$68.4^{\pm 0.17}$	$57.2^{\pm 0.06}$
AlphaNet ($\rho = 1.75$)	$37.7^{\pm 0.89}$	$53.7^{\pm 0.14}$	$68.4^{\pm 0.10}$	$57.2^{\pm 0.05}$
AlphaNet ($\rho = 2$)	$37.1^{\pm 0.98}$	$53.8^{\pm 0.12}$	$68.5^{\pm 0.11}$	$57.2^{\pm 0.06}$
AlphaNet ($\rho = 3$)	$34.5^{\pm 1.23}$	$54.3^{\pm 0.14}$	$68.8^{\pm 0.11}$	$57.2^{\pm 0.08}$

Table A3: AlphaNet with RIDE baseline on ImageNet-LT.

Experiment	Few	Med.	Many	Overall
Baseline	24.9	37.6	42.0	36.7
AlphaNet ($\rho = 0.1$)	$38.2^{\pm 1.30}$	$30.4^{\pm 0.84}$	$37.3^{\pm 0.72}$	$34.4^{\pm 0.41}$
AlphaNet ($\rho = 0.2$)	$34.8^{\pm 1.42}$	$32.4^{\pm 0.66}$	$39.0^{\pm 0.29}$	$35.3^{\pm 0.15}$
AlphaNet ($\rho = 0.25$)	$34.4^{\pm 1.27}$	$32.8^{\pm 0.82}$	$39.3^{\pm 0.34}$	$35.5^{\pm 0.29}$
AlphaNet ($\rho = 0.3$)	$33.2^{\pm 1.57}$	$33.4^{\pm 0.75}$	$39.5^{\pm 0.60}$	$35.6^{\pm 0.25}$
AlphaNet ($\rho = 0.4$)	$32.4^{\pm 1.47}$	$33.8^{\pm 0.69}$	$39.8^{\pm 0.46}$	$35.7^{\pm 0.22}$
AlphaNet ($\rho = 0.5$)	$31.0^{\pm 0.88}$	$34.5^{\pm 0.17}$	$40.4^{\pm 0.29}$	$35.9^{\pm 0.09}$
AlphaNet ($\rho = 0.75$)	$28.6^{\pm 1.27}$	$35.5^{\pm 0.40}$	$41.0^{\pm 0.13}$	$36.1^{\pm 0.11}$
AlphaNet ($\rho = 1$)	$27.0^{\pm 1.02}$	$36.1^{\pm 0.31}$	$41.3^{\pm 0.13}$	$36.2^{\pm 0.10}$
AlphaNet ($\rho = 1.25$)	$26.9^{\pm 1.23}$	$36.0^{\pm 0.47}$	$41.3^{\pm 0.14}$	$36.1^{\pm 0.16}$
AlphaNet ($\rho = 1.5$)	$25.5^{\pm 0.89}$	$36.5^{\pm 0.36}$	$41.6^{\pm 0.21}$	$36.2^{\pm 0.11}$
AlphaNet ($\rho = 1.75$)	$25.4^{\pm 1.32}$	$36.5^{\pm 0.29}$	$41.5^{\pm 0.23}$	$36.2^{\pm 0.11}$
AlphaNet ($\rho = 2$)	$24.9^{\pm 1.38}$	$36.6^{\pm 0.49}$	$41.5^{\pm 0.20}$	$36.1^{\pm 0.10}$
AlphaNet ($\rho = 3$)	$22.3^{\pm 1.56}$	$37.3^{\pm 0.28}$	$41.9^{\pm 0.20}$	$36.1^{\pm 0.14}$

Table A4: AlphaNet with cRT baseline on Places-LT.

Experiment	Few	Med.	Many	Overall
Baseline	28.7	39.1	40.6	37.6
AlphaNet ($\rho = 0.1$)	$42.5^{\pm 1.03}$	$29.5^{\pm 1.01}$	$34.4^{\pm 0.94}$	$33.8^{\pm 0.58}$
AlphaNet ($\rho = 0.2$)	$41.3^{\pm 1.30}$	$31.0^{\pm 0.81}$	$35.5^{\pm 0.81}$	$34.6^{\pm 0.44}$
AlphaNet ($\rho = 0.25$)	$40.5^{\pm 2.25}$	$30.9^{\pm 2.92}$	$35.6^{\pm 2.20}$	$34.4^{\pm 1.67}$
AlphaNet ($\rho = 0.3$)	$38.7^{\pm 1.13}$	$33.2^{\pm 1.12}$	$37.0^{\pm 0.70}$	$35.6^{\pm 0.51}$
AlphaNet ($\rho = 0.4$)	$38.0^{\pm 1.45}$	$33.6^{\pm 1.18}$	$37.3^{\pm 0.65}$	$35.8^{\pm 0.50}$
AlphaNet ($\rho = 0.5$)	$37.1^{\pm 1.39}$	$34.4^{\pm 0.80}$	$37.7^{\pm 0.52}$	$36.1^{\pm 0.31}$
AlphaNet ($\rho = 0.75$)	$35.5^{\pm 1.25}$	$35.3^{\pm 0.59}$	$38.5^{\pm 0.28}$	$36.5^{\pm 0.16}$
AlphaNet ($\rho = 1$)	$34.6^{\pm 0.97}$	$35.8^{\pm 0.54}$	$38.6^{\pm 0.39}$	$36.6^{\pm 0.22}$
AlphaNet ($\rho = 1.25$)	$32.6^{\pm 1.28}$	$36.8^{\pm 0.60}$	$39.3^{\pm 0.39}$	$36.9^{\pm 0.19}$
AlphaNet ($\rho = 1.5$)	$32.2^{\pm 1.17}$	$37.2^{\pm 0.36}$	$39.5^{\pm 0.39}$	$37.0^{\pm 0.11}$
AlphaNet ($\rho = 1.75$)	$31.7^{\pm 1.35}$	$37.3^{\pm 0.43}$	$39.5^{\pm 0.27}$	$37.0^{\pm 0.09}$
AlphaNet ($\rho = 2$)	$30.9^{\pm 1.28}$	$37.6^{\pm 0.40}$	$39.8^{\pm 0.18}$	$37.1^{\pm 0.14}$
AlphaNet ($\rho = 3$)	$27.8^{\pm 1.94}$	$38.5^{\pm 0.51}$	$40.2^{\pm 0.29}$	$37.1^{\pm 0.10}$

Table A5: AlphaNet with LWS baseline on Places-LT.

Experiment	Few	Med.	Many	Overall
Baseline	25.8	52.1	69.3	50.2
AlphaNet ($\rho = 0.1$)	$38.2^{\pm 3.22}$	$38.1^{\pm 5.01}$	$56.3^{\pm 7.65}$	$44.5^{\pm 3.50}$
AlphaNet ($\rho = 0.2$)	$36.0^{\pm 4.34}$	$41.4^{\pm 5.41}$	$59.1^{\pm 8.31}$	$45.9^{\pm 3.58}$
AlphaNet ($\rho = 0.25$)	$34.0^{\pm 1.70}$	$44.1^{\pm 1.68}$	$62.6^{\pm 1.54}$	$47.6^{\pm 0.76}$
AlphaNet ($\rho = 0.3$)	$32.9^{\pm 1.20}$	$45.3^{\pm 1.02}$	$64.0^{\pm 0.78}$	$48.1^{\pm 0.51}$
AlphaNet ($\rho = 0.4$)	$31.1^{\pm 1.27}$	$45.6^{\pm 1.63}$	$64.8^{\pm 1.22}$	$48.0^{\pm 0.84}$
AlphaNet ($\rho = 0.5$)	$30.9^{\pm 1.82}$	$47.0^{\pm 1.25}$	$65.7^{\pm 0.94}$	$48.7^{\pm 0.41}$
AlphaNet ($\rho = 0.75$)	$28.6^{\pm 1.63}$	$48.3^{\pm 0.84}$	$66.6^{\pm 0.65}$	$48.8^{\pm 0.26}$
AlphaNet ($\rho = 1$)	$27.2^{\pm 1.69}$	$49.1^{\pm 0.85}$	$67.4^{\pm 0.62}$	$48.9^{\pm 0.30}$
AlphaNet ($\rho = 1.25$)	$26.1^{\pm 1.54}$	$49.8^{\pm 0.59}$	$68.0^{\pm 0.47}$	$49.1^{\pm 0.42}$
AlphaNet ($\rho = 1.5$)	$25.0^{\pm 1.15}$	$50.1^{\pm 1.12}$	$67.9^{\pm 1.01}$	$48.8^{\pm 0.63}$
AlphaNet ($\rho = 1.75$)	$24.8^{\pm 1.09}$	$50.3^{\pm 0.61}$	$68.4^{\pm 0.33}$	$49.0^{\pm 0.27}$
AlphaNet ($\rho = 2$)	$24.3^{\pm 1.74}$	$51.0^{\pm 0.55}$	$68.9^{\pm 0.47}$	$49.2^{\pm 0.34}$
AlphaNet ($\rho = 3$)	$22.2^{\pm 1.71}$	$51.6^{\pm 0.86}$	$69.3^{\pm 0.58}$	$49.0^{\pm 0.31}$

Table A6: AlphaNet with RIDE baseline on CIFAR-100-LT.

Experiment	Few	Med.	Many	Overall
Baseline	33.6	49.4	69.7	51.8
AlphaNet ($\rho = 0.1$)	$40.9^{\pm 4.12}$	$37.4^{\pm 7.63}$	$62.1^{\pm 5.07}$	$47.1^{\pm 3.27}$
AlphaNet ($\rho = 0.2$)	$42.6^{\pm 2.47}$	$32.9^{\pm 4.98}$	$58.7^{\pm 3.36}$	$44.8^{\pm 2.43}$
AlphaNet ($\rho = 0.25$)	$42.3^{\pm 2.45}$	$34.4^{\pm 6.36}$	$59.5^{\pm 4.83}$	$45.5^{\pm 3.31}$
AlphaNet ($\rho = 0.3$)	$40.9^{\pm 3.77}$	$36.6^{\pm 6.76}$	$61.3^{\pm 4.78}$	$46.6^{\pm 3.14}$
AlphaNet ($\rho = 0.4$)	$42.3^{\pm 1.73}$	$33.1^{\pm 6.20}$	$58.9^{\pm 4.24}$	$44.9^{\pm 3.25}$
AlphaNet ($\rho = 0.5$)	$43.2^{\pm 1.17}$	$32.1^{\pm 4.73}$	$58.7^{\pm 3.55}$	$44.7^{\pm 2.64}$
AlphaNet ($\rho = 0.75$)	$43.1^{\pm 1.45}$	$31.3^{\pm 5.14}$	$57.7^{\pm 4.01}$	$44.1^{\pm 2.95}$
AlphaNet ($\rho = 1$)	$42.5^{\pm 2.31}$	$31.3^{\pm 6.45}$	$57.4^{\pm 4.50}$	$43.8^{\pm 3.21}$
AlphaNet ($\rho = 1.25$)	$41.7^{\pm 4.03}$	$33.4^{\pm 8.11}$	$59.1^{\pm 5.61}$	$44.9^{\pm 3.91}$
AlphaNet ($\rho = 1.5$)	$43.6^{\pm 0.87}$	$31.3^{\pm 3.49}$	$57.8^{\pm 2.57}$	$44.3^{\pm 1.95}$
AlphaNet ($\rho = 1.75$)	$42.7^{\pm 0.70}$	$30.0^{\pm 4.75}$	$56.5^{\pm 3.51}$	$43.1^{\pm 2.93}$
AlphaNet ($\rho = 2$)	$43.1^{\pm 0.79}$	$28.4^{\pm 1.86}$	$55.4^{\pm 1.59}$	$42.2^{\pm 1.39}$
AlphaNet ($\rho = 3$)	$43.2^{\pm 0.93}$	$28.0^{\pm 2.00}$	$55.3^{\pm 1.45}$	$42.1^{\pm 1.43}$

Table A7: AlphaNet with LTR baseline on CIFAR-100-LT.

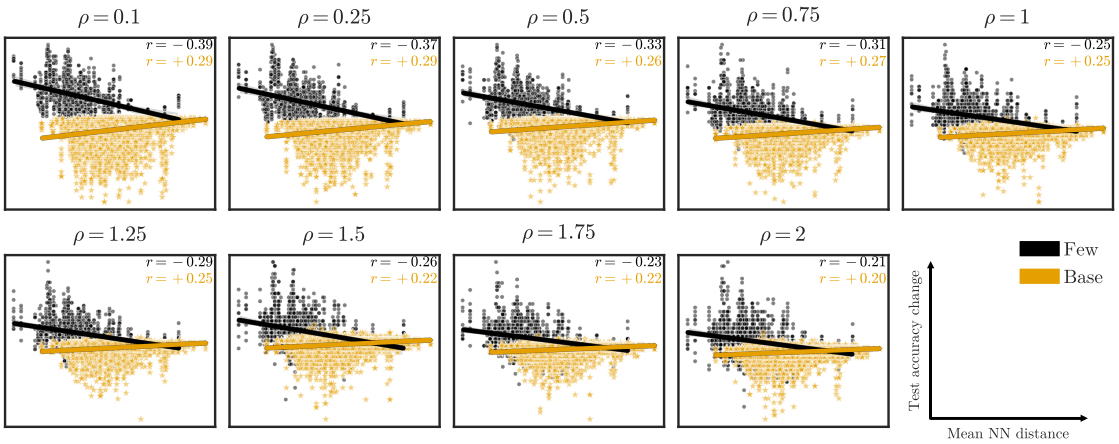

Figure A4: ...

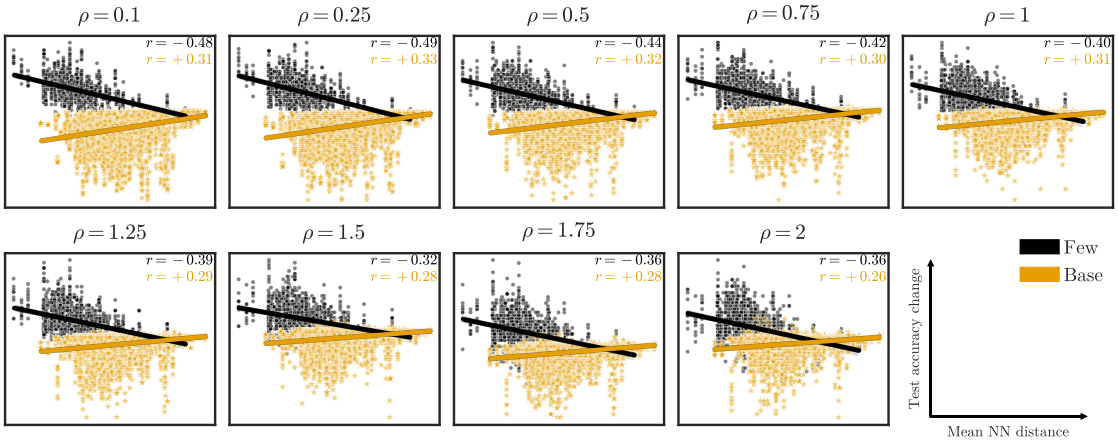

Figure A5: ...

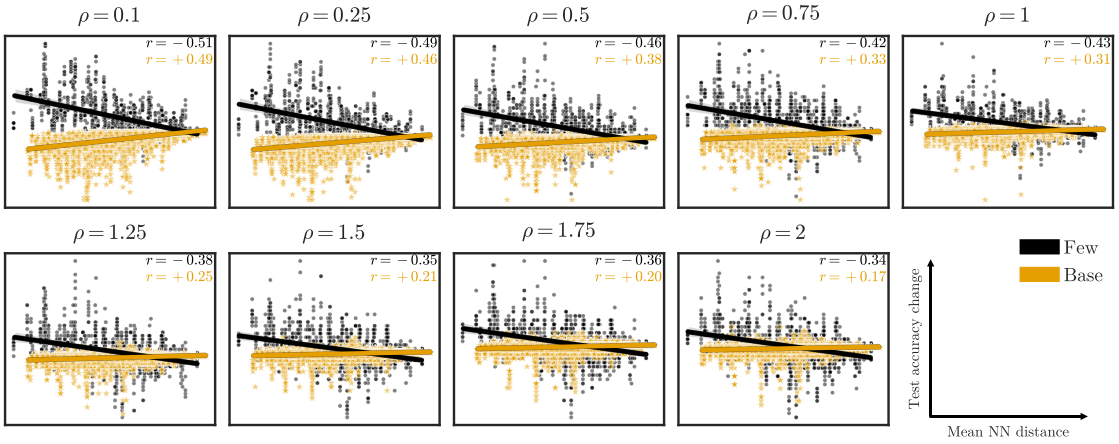

Figure A6: ...

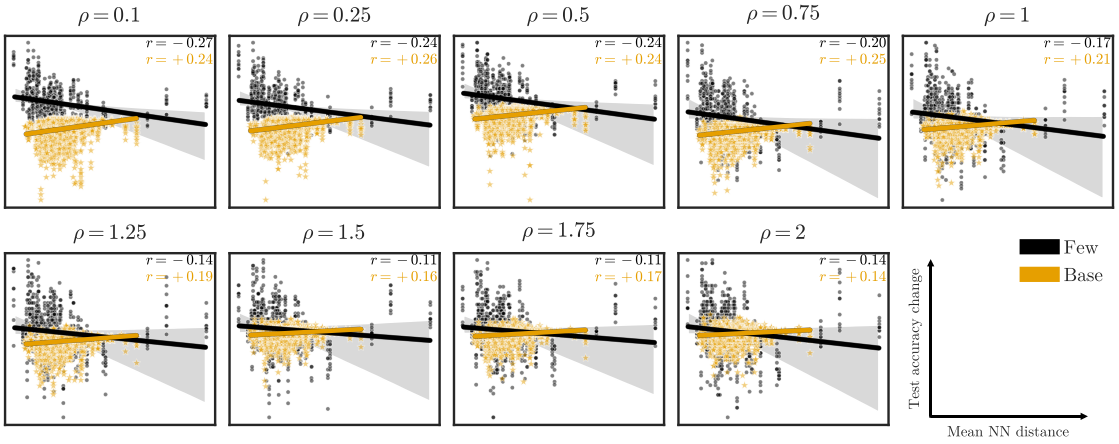

Figure A7: ...

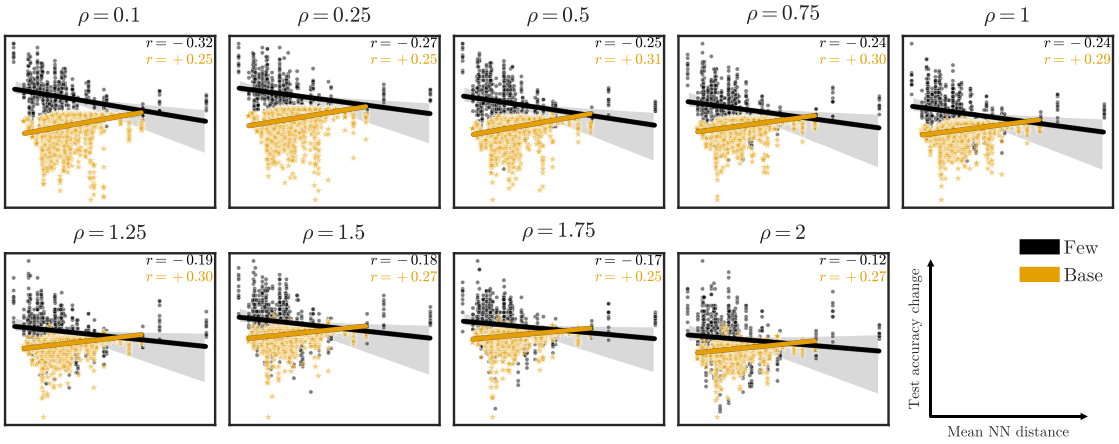

Figure A8: ...

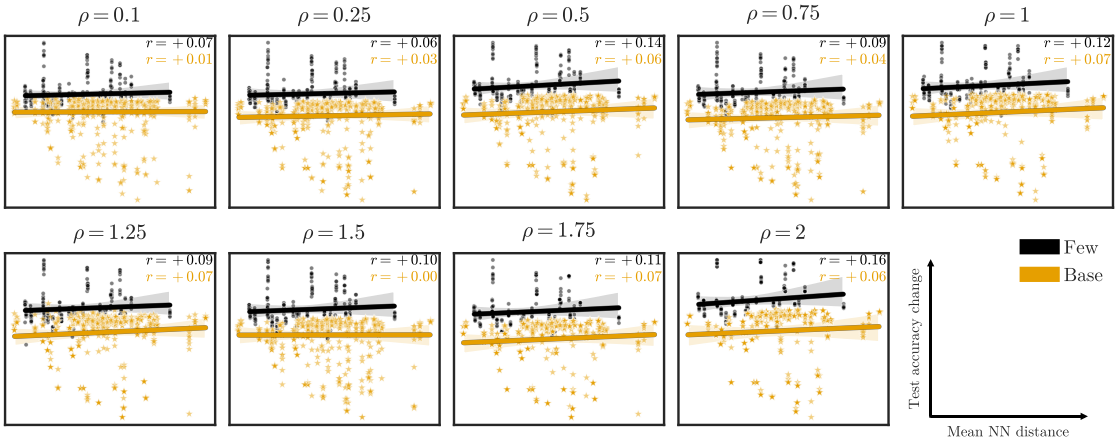

Figure A9: ...

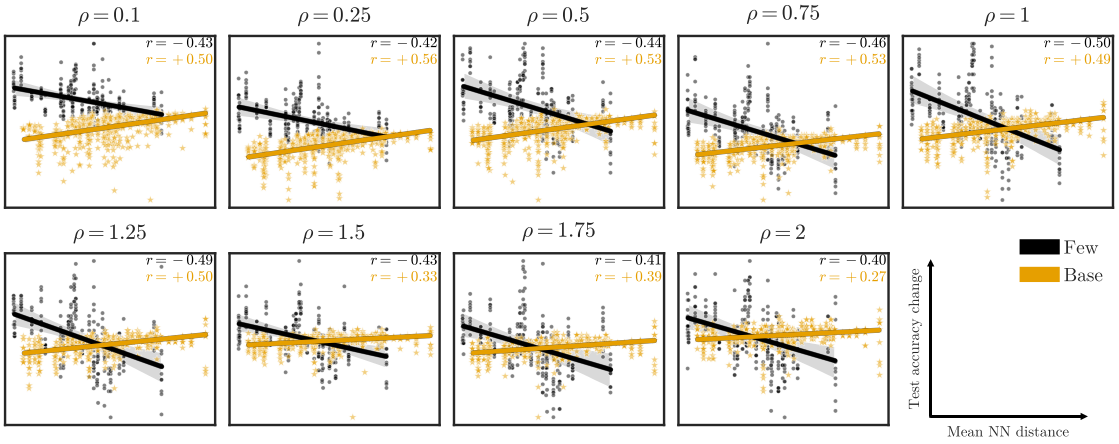

Figure A10: ...

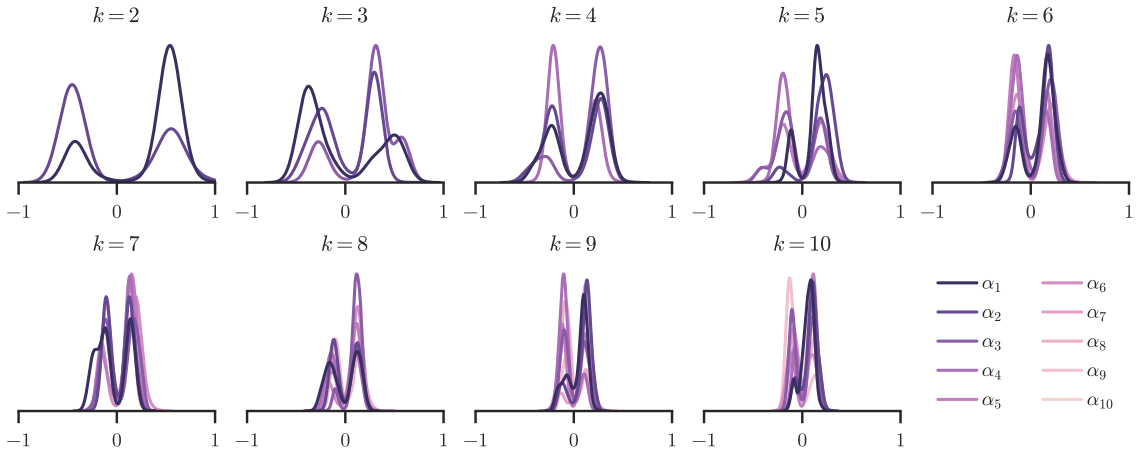

Figure A11: ...

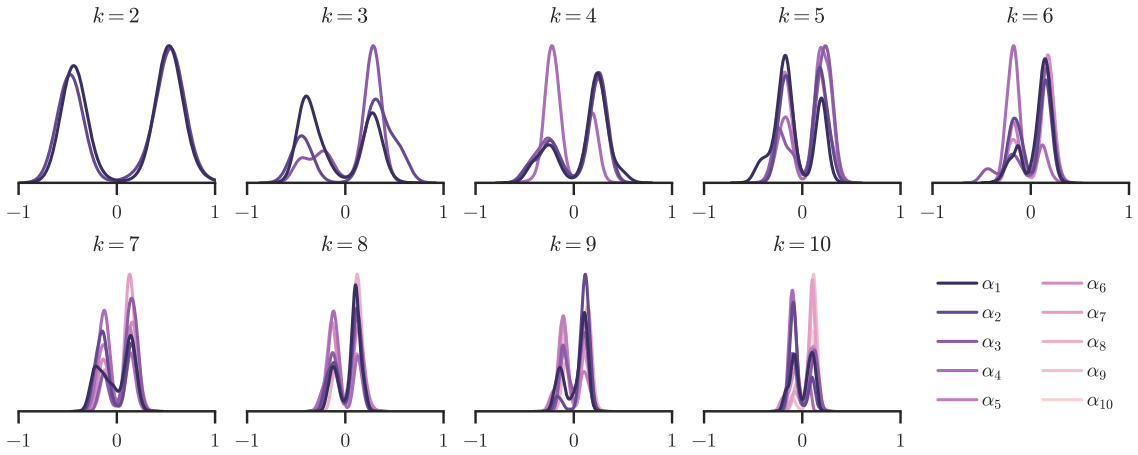

Figure A12: ...

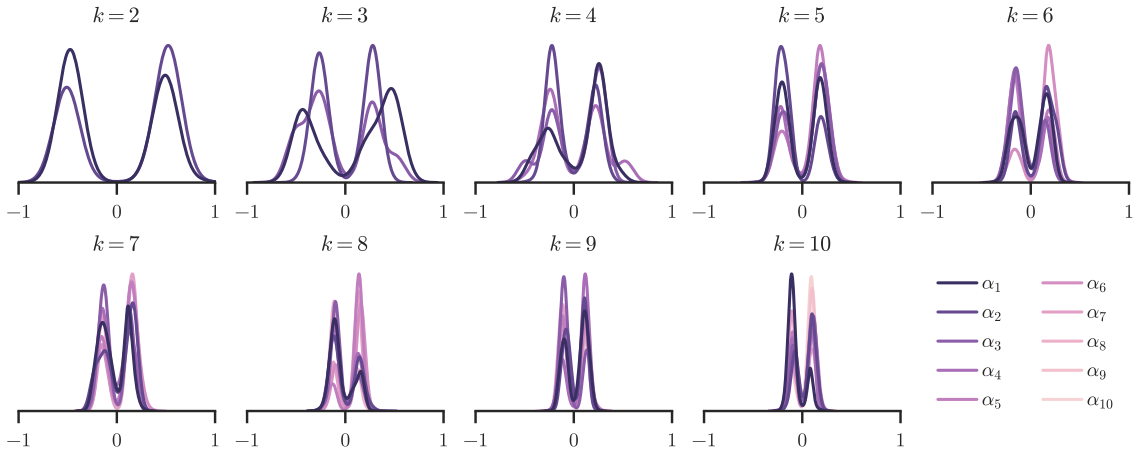

Figure A13: ...

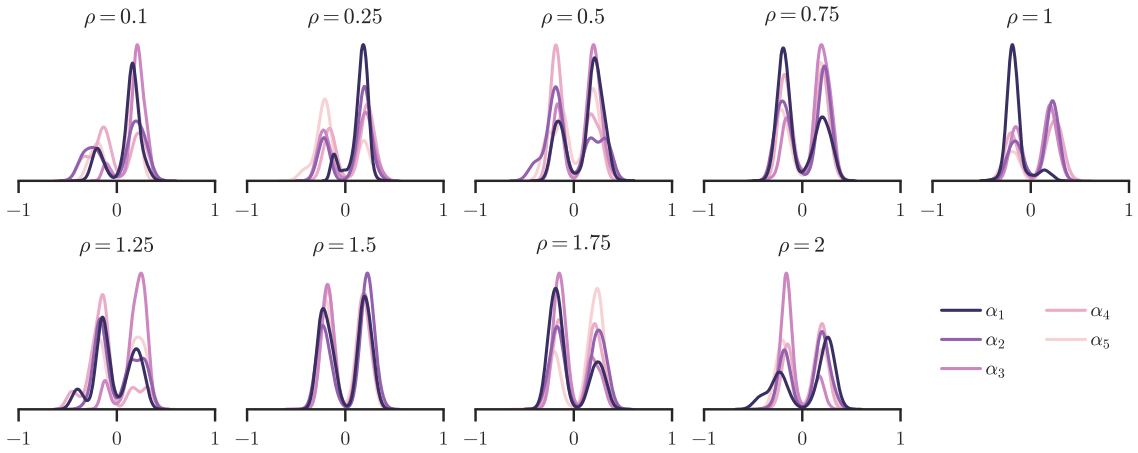

Figure A14: ...

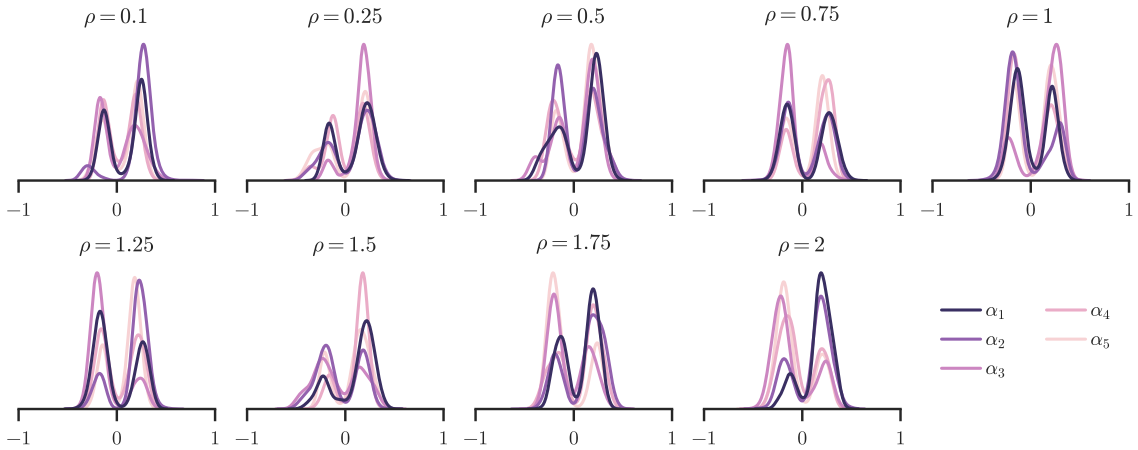

Figure A15: ...

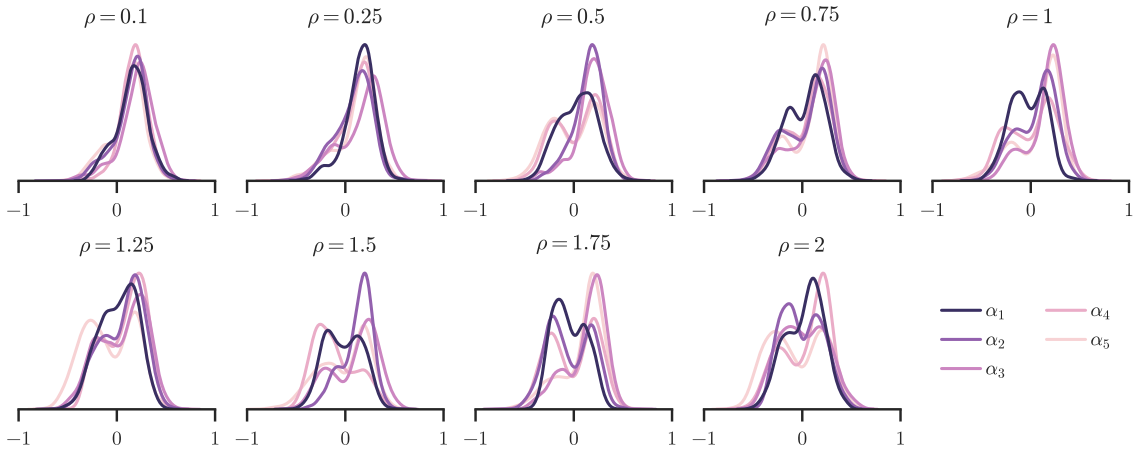

Figure A16: ...

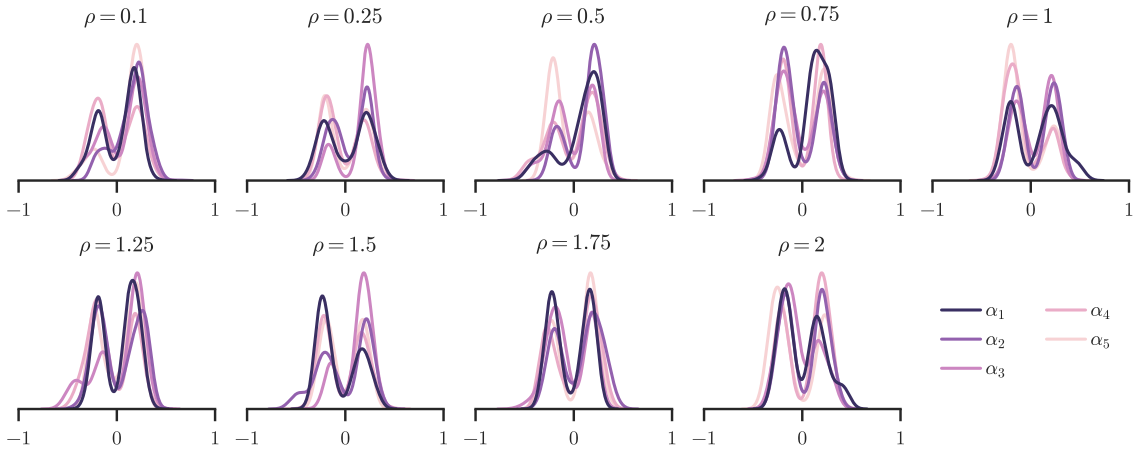

Figure A17: ...

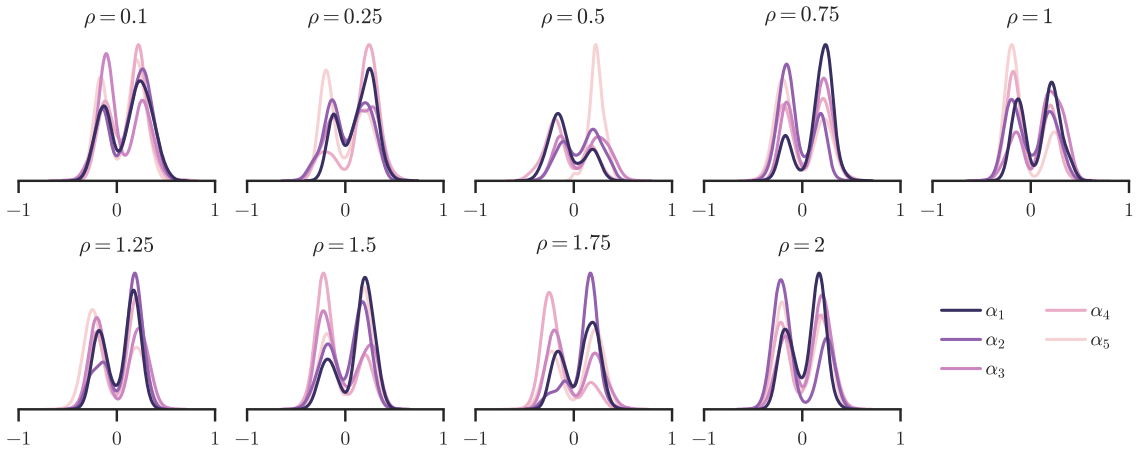

Figure A18: ...

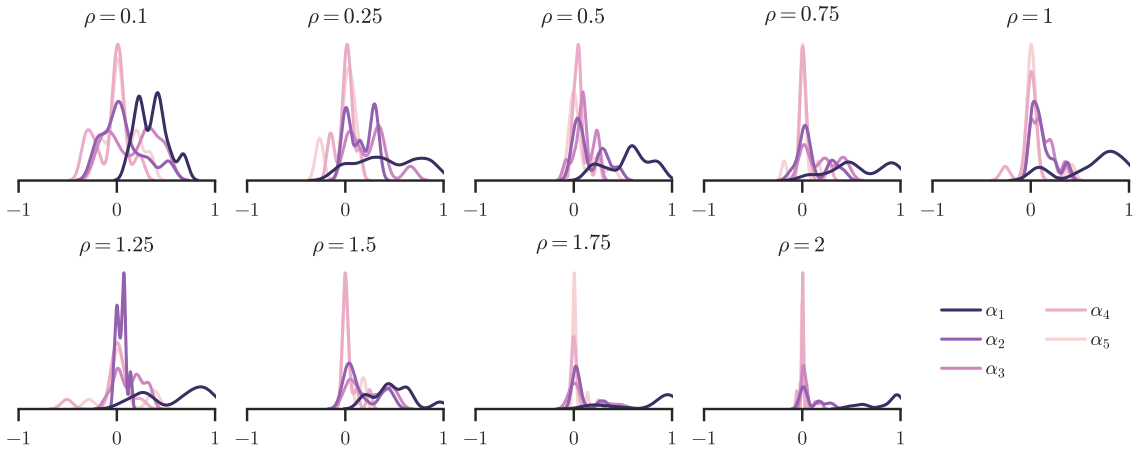

Figure A19: ...

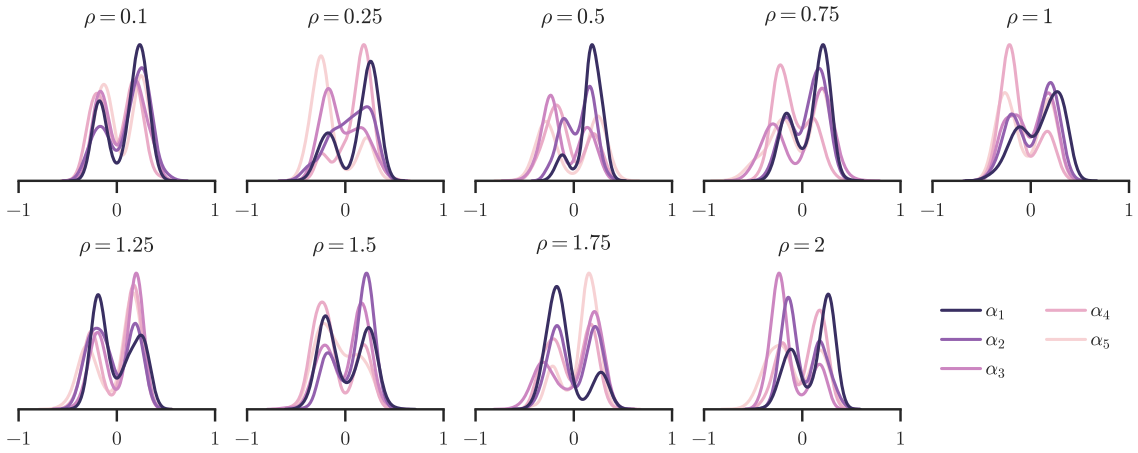

Figure A20: ...